

Journal of Materials Chemistry B

Accepted Manuscript



This is an *Accepted Manuscript*, which has been through the Royal Society of Chemistry peer review process and has been accepted for publication.

Accepted Manuscripts are published online shortly after acceptance, before technical editing, formatting and proof reading. Using this free service, authors can make their results available to the community, in citable form, before we publish the edited article. We will replace this *Accepted Manuscript* with the edited and formatted *Advance Article* as soon as it is available.

You can find more information about *Accepted Manuscripts* in the [Information for Authors](#).

Please note that technical editing may introduce minor changes to the text and/or graphics, which may alter content. The journal's standard [Terms & Conditions](#) and the [Ethical guidelines](#) still apply. In no event shall the Royal Society of Chemistry be held responsible for any errors or omissions in this *Accepted Manuscript* or any consequences arising from the use of any information it contains.

1 **Encapsulation of VEGF₁₆₅ in magnetic PLGA nanocapsules for potential local**
2 **delivery and bioactivity into human brain endothelial cells**

3
4 E. Carenza¹, O. Jordan², P. Martínez-San Segundo³, R. Jiřík⁴, Z. Starčuk jr.⁴, G. Borchard², A.
5 Rosell^{3*}, A. Roig^{1*}.

6 *Corresponding authors and equal contribution

7
8 Anna Roig

9 e-mail: roig@icmab.es

10 Institut de Ciència de Materials de Barcelona (ICMAB-CSIC)

11 Campus de la UAB

12 08193 Bellaterra (Barcelona), SPAIN

13

14 Anna Rosell

15 e-mail: anna.rosell@vhir.org

16 Neurovascular Research Laboratory and Neurovascular Unit,

17 Vall d'Hebron Institut de Recerca, Passeig Vall d'Hebron, 119-129,

18 08035 Barcelona, SPAIN

19

20 ¹ Institut de Ciència de Materials de Barcelona, Consejo Superior de Investigaciones Científicas
21 (ICMAB-CSIC), Campus de la UAB, 08193 Bellaterra, Catalunya, Spain.

22 ² School of Pharmaceutical Sciences, University of Geneva, Quai Ernest Ansermet 30, 1205
23 Genève, Switzerland.

24 ³ Neurovascular Research Laboratory and Neurovascular Unit, Vall d'Hebron Institut de Recerca,
25 Universitat Autònoma de Barcelona; Passeig Vall d'Hebron, 119-129 Barcelona, 08035
26 Catalunya, Spain.

27 ⁴ Institute of Scientific Instruments, Academy of Sciences of the Czech Republic, Královopolská
28 147, 612 64 Brno, Czech Republic.

29

30 **Abstract:**

31

32 Angiogenesis is an important repairing mechanism in response to ischemia. The

33 administration of pro-angiogenic proteins is an attractive therapeutic strategy to enhance

34 angiogenesis after an ischemic event. Their labile structures and short circulation times *in*

35 *vivo* are the main obstacles that reduce the bioactivity and dosage of such proteins at the

36 target site. We report on poly(D,L-lactic-co-glycolic acid) (PLGA) nanocapsules

37 (diameter < 200 nm) containing bioactive vascular endothelial growth factor-165

38 (VEGF₁₆₅) in the inner core and superparamagnetic iron oxide nanoparticles (SPIONs)

39 embedded in the polymeric shell. The system showed good encapsulation efficiencies for

40 both VEGF₁₆₅ and the SPIONs and a sustained protein release over 14 days. *In vitro*

41 studies confirmed protein bioactivity in the form of a significantly increased proliferation
42 in human microvascular brain endothelial cell cultures once the protein was released.
43 Through magnetic resonance imaging (MRI) measurements we demonstrated excellent T_2
44 contrast image properties with r_2 values as high as $213 \text{ mM}^{-1} \text{ s}^{-1}$. In addition, magnetic
45 VEGF₁₆₅-loaded PLGA nanocapsules could be displaced and accumulated under an
46 external magnetic field for guiding and retention purposes. We therefore suggest that
47 VEGF₁₆₅-loaded magnetic PLGA nanocapsules may become a new targeted protein-
48 delivery strategy in the development of future pro-angiogenic treatments, as for instance
49 those directed to neurorepair after an ischemic event.

50

51 **Introduction**

52 Angiogenesis, the formation of new blood vessels from pre-existing ones, is an important
53 repairing mechanism in response to ischemia. It is increasingly being established that
54 angiogenesis enhancement, after an ischemia event, facilitate patient recovery. The
55 administration of pro-angiogenic proteins is an attractive therapeutic strategy to enhance
56 local angiogenesis^{1,2}. Several approaches are under investigation to achieve efficient and
57 non-invasive local angiogenic treatments³. One of the most frequently used approaches
58 consists of encapsulating pro-angiogenic proteins into suitable polymeric micro-^{4,5,6} or
59 nano-carriers^{7,8} which may preserve protein structure and allow local delivery with
60 reduced off-target effects. Recombinant human vascular endothelial growth factor-165
61 (VEGF₁₆₅) is one of the most studied pro-angiogenic growth factors⁹ and it has been
62 encapsulated with high encapsulation efficiencies into poly(D,L-lactic-co-glycolic acid)
63 (PLGA) microspheres⁵ and nanocapsules^{7,10}. Importantly, evidence of angiogenesis
64 induced by the delivery of VEGF₁₆₅ from PLGA carriers has also been provided by *in*
65 *vivo* assays, which show tissue revascularization and recovery in animal models of hind-
66 limb ischemia^{11,12,13}.

67 The use of magnetic materials to assist on-site delivery of therapeutic agents, with an
68 external magnetic field, has raised considerable interest. There have been several studies
69 on the encapsulation of superparamagnetic iron oxide nanoparticles (SPIONs) into PLGA
70 particles^{14,15,16} together with drugs (*e.g.*, anti-cancer and anti-arthritis molecules), for
71 targeted drug delivery purposes and for use in non-invasive imaging (by magnetic
72 resonance imaging, MRI) of tissues^{17,18,19,20,21}. On the other hand, there are only a few
73 examples of the co-encapsulation of SPIONs with proteins^{22,23} and to date, VEGF has
74 only been encapsulated into PLGA particles with gadolinium complexes²⁴. The lack of
75 published research on protein–SPION co-encapsulation could be related to the labile
76 structure of proteins and to their potential inactivation after adsorption on the surface of
77 SPIONs²⁵. In fact, protein adsorption may induce conformational changes of the native
78 structure with the exposure of novel epitopes that may transmit different biological
79 signals²⁶.

80 Here, we report on the co-encapsulation of recombinant human VEGF₁₆₅ and SPIONs
81 using a double emulsion-solvent evaporation method. In this process, VEGF₁₆₅ has been
82 encapsulated in the inner core of a PLGA nanocapsule, whilst hydrophobic oleic-acid-
83 coated SPIONs have been embedded in the organic polymer phase. Our purpose is to
84 demonstrate that, by confining VEGF₁₆₅ and SPIONs in two different compartments of the carrier,
85 protein bioactivity is preserved and that the magnetic nanocapsules can be externally guided in
86 presence of a suitable magnetic field.

87

88 **Materials and Methods**

89 **Nanocapsule synthesis**

90 In a small propylene tube, an organic phase containing PLGA and SPIONs was prepared
91 as follows: 50 mg of PLGA 50:50 (RG502 Boehringer Ingelheim, $M_w = 18000$ Da,
92 inherent viscosity 0.16–0.24 dL g⁻¹) were mixed with 0.45 mL of dichloromethane

93 (Sigma Aldrich) by using an ultrasonic bath. Oleic-acid-coated SPIONs (0.94 mg) were
94 dispersed in 50 μL of dichloromethane and then mixed with the polymer solution in an
95 ultrasonic bath.

96 25 μg of lyophilized recombinant human VEGF₁₆₅ (Peprotech) dissolved in 50 μL of
97 EBM (endothelial basal medium, Lonza) were added in one drop to the organic phase.
98 The first emulsion was obtained by sonicating at 240 W for 28 s (Vibra-cell® VCX 500,
99 Sonics & Materials). The temperature during the whole emulsion process was kept at 4
100 °C by use of an ice bath. The second emulsion was prepared by adding 2 mL of 2% w/v
101 polyvinyl alcohol (PVAL, Sigma Aldrich) aqueous solution and sonicating for additional
102 28 s. The as-formed colloidal suspension was poured into 50 mL of MilliQ water and kept
103 under mechanical stirring at room temperature for 2 h to allow complete evaporation of
104 the organic solvent. Then the colloidal dispersion was washed with MilliQ water three
105 times with centrifugations at $9469 \times g$ (centrifuge Allegra® 64R Beckman), each time with
106 addition of fresh water, to reduce the amount of PVAL adsorbed on the PLGA. Finally,
107 the particles were re-dispersed in an aqueous solution containing 0.2% w/v trehalose
108 (Sigma Aldrich) before freeze-drying at -80 °C for 2 days. The as-obtained powder was
109 stored at 4 °C with desiccant silica gel.

110

111 **Experimental methods**

112 Dynamic light scattering (DLS)

113 Particle hydrodynamic diameter was measured by re-dispersion of 0.6 mg of lyophilized
114 powder into 1 mL of MilliQ water. Measurements were performed with a Zetasizer Nano
115 ZS from Malvern Instruments equipped with a He/Ne 633 nm laser using a disposable
116 plastic cuvette. Size measurements were run in triplicate, each for 15 scans, at 25°C. Zeta
117 potential measurements were run three times at 25°C.

118

119 Scanning electron microscopy (SEM)

120 2 mg of the lyophilized powder were re-dispersed into 600 μL of MilliQ water and
121 centrifuged twice at $1073 \times g$ for 20 min. Each time the supernatant was discarded and
122 fresh water added. Finally, particles were re-dispersed in 1 mL of water and one drop of
123 the slightly turbid suspension was deposited onto a small slice of silicon wafer stuck on
124 top of a carbon layer. The sample was dried at room temperature and then covered with 2
125 nm of Au-Pd (Emitech K550 Sputter Coater, 25 mA for 1 min). Images were acquired
126 under high vacuum, with a FESEM Merlin, Zeiss using frame-scan modality, repeated 15
127 times.

128

129 Cryo-transmission electron microscopy (Cryo-TEM)

130 Cryo-TEM experiments were performed on aqueous suspensions of nanoparticles at a
131 concentration of 1 mg mL^{-1} . After one washing with MilliQ water by using a
132 centrifugation at $1073 \times g$ for 20 min (centrifuge Minispin[®], Eppendorf[®]), a drop of
133 suspension was placed onto a Quantifoil[®] grid where a perforated foil was used to bear
134 an ultra-thin carbon support foil to minimize the total specimen thickness. The drop was
135 blotted with filter paper and the grid was quenched rapidly into liquid ethane to produce
136 vitreous ice, avoiding the formation of crystals. The grid was then transferred into the
137 TEM microscope (JEM-2011 operating at 200 kV), where the temperature was kept under
138 $-140 \text{ }^\circ\text{C}$ by use of liquid nitrogen during the imaging.

139

140 Superconductive quantum interference device (SQUID)

141 A magnetometer from Quantum Design MPMS5XL was used to perform magnetization
142 measurements of SPIONs. A gelatin capsule was filled with 3 mg of lyophilized powder
143 together with some cotton to reduce sample movement during measurements with applied
144 magnetic field. The as-prepared sample was inserted into the SQUID magnetometer

145 sample holder. The amount of encapsulated SPIONs was evaluated as follows: initially,
146 the remnant magnetization value of the magnetized nanocapsules ($M_{R \text{ nanocapsule}}$) was
147 measured at 5 K after the material was magnetized at 5 T and this value (emu) was
148 divided by the weight of the analyzed powder (emu/ g_{nanocapsule}). Subsequently, the
149 remnant magnetization per gram of nanocapsule (emu/g_{nanocapsule}) was divided by the
150 remnant magnetization per gram of SPIONs (emu/g_{Fe2O3}) measured at the same
151 conditions giving the average amount of magnetic material inside a nanocapsule (g_{Fe2O3}/
152 g_{nanocapsule}). The as-obtained “experimental SPION loading” was divided by the “nominal
153 SPION loading” to calculate SPION encapsulation efficiency, as follows:

$$154 \quad EE\% = \frac{\text{experimental SPIONs loading}}{\text{nominal SPIONs loading}} \times 100$$

155

156 Magnetic resonance imaging (MRI)

157 Phantoms were prepared by filling 2.5 mL microtubes with a solution of 1.5% agarose in
158 water, into which different amounts of nanocapsules had been admixed. Such a set of
159 phantoms spanning the iron dose range from 0 to 15 $\mu\text{g mL}^{-1}$ was prepared with four
160 different batches of synthesized nanocapsules. Agarose phantoms were kept at 4 °C until
161 imaged in a 9.4 T MR system (BioSpin 94/30, Bruker BioSpin, Ettlingen, Germany) by
162 using a quadrature 86 mm inner-diameter volume coil as follows: To determine T_2
163 relaxation times in each phantom, a series of T_2 weighted images were acquired with a
164 multi-slice multi-echo (MSME) sequence, with TR = 3 s, 30 TE values from 11 to 330 ms
165 (11 ms echo spacing), matrix size = 256 × 256, field of view (FOV) = 65 × 65 mm, and
166 slice thickness = 1.5 mm (four adjacent slices). Quantitative T_2 values were obtained from
167 hand-drawn regions of interest by using curve fitting in the Image Sequence Analysis
168 (ISA) Tool (ParaVision v.5.1, Bruker BioSpin, Ettlingen, Germany).

169

170 Total VEGF₁₆₅ determination by enzyme-linked immunosorbent assay (ELISA)

171 Low-weight Eppendorf pipettes (Eppendorf®) were used for the following experiments:
172 Three independent batches of nanocapsules loaded with VEGF₁₆₅ and SPIONs were
173 analyzed simultaneously with PGLA nanocapsules loaded with SPIONs only (control).
174 Lyophilized nanocapsules (5 mg) were previously sterilized under UV rays for 18 h²⁷. To
175 determine VEGF₁₆₅ encapsulation efficiency, nanocapsules were dissolved at a
176 concentration of 10 mg mL⁻¹ in an aqueous solution of 0.1 M NaOH, 10% dimethyl
177 sulfoxide (DMSO), 0.2% w/v sodium dodecyl sulfate (SDS), under magnetic stirring²⁸.
178 The as-obtained samples were centrifuged at 13226 × g for 5 min to precipitate SPIONs.
179 The collected supernatants were stored at -80 °C until used to determine total VEGF₁₆₅
180 content by ELISA (Quantikine® ELISA human VEGF immunoassay, catalog number
181 DVE00, R&D Systems).

182 In parallel, to measure the amount of VEGF₁₆₅ released from nanocapsules, sterilized
183 lyophilized samples (5 mg from each batch) were dispersed at a concentration of 10 mg
184 mL⁻¹ in a release medium consisting of 0.1% w/v bovine serum albumin (BSA) and 1%
185 penicillin–streptomycin in phosphate-buffered saline (PBS 1X). Subsequently, all
186 samples were placed in a water bath (37 °C) with horizontal shaking (80 oscillations per
187 minute). Aliquots of 0.1 mL were taken after 1 and 6 h, 2, 6, and 14 days, centrifuged at
188 13226 × g for 5 min and the supernatant was stored at -80 °C until used for measuring
189 VEGF₁₆₅ content by the Quantikine® ELISA (R&D Systems). The volume of the aqueous
190 suspensions was kept constant during the release study by adding fresh release medium.
191 VEGF₁₆₅ concentration (pg mL⁻¹) was measured by colorimetric absorption at
192 wavelengths of 450 nm and 540 nm. All samples were run in duplicate and mean values
193 were used (coefficient of variation between duplicates was less than 20%).

194

195

196 *In vitro* VEGF₁₆₅ bioactivity

197 VEGF-containing and control samples obtained during the release study were used to
198 assess protein bioactivity. Briefly, supernatants stored at -80°C were thawed and five
199 samples corresponding to the different times of analyzed release (1 and 6 h, 2, 6, and 14
200 days), were obtained by pooling three batches (RG502_23, 24, and 25, see Table 1).
201 Supernatants of VEGF-free nanocapsules (batch RG502_27) collected at different times
202 were used as the control medium.

203 Human cerebral microvascular endothelial cells (hCMEC/D3)²⁹ were used to assess the
204 activity of encapsulated and released VEGF by measuring cell proliferation and viability.
205 Briefly, 2.5×10^3 cells were seeded in 24-well-plates in endothelial cell growth media,
206 (EGM-2, Lonza) containing endothelial basal media (EBM) plus supplements: VEGF,
207 insulin-like growth factor, bovine FGF, hydrocortisone, ascorbate, and 2% fetal bovine
208 serum (FBS). After four days in culture, cells were thoroughly washed with phosphate-
209 buffered saline (PBS 1X) and treated with pooled VEGF media to a final concentration of
210 10 ng mL^{-1} of VEGF (according to the ELISA results). This concentration has been
211 shown by other authors to induce *in vitro* proliferation of endothelial cells³⁰. Two controls
212 were run in each experiment: EBM and medium of batch RG502_27 (release control).
213 EBM was used to load all wells to a final volume of 0.4 mL. After 48 h of treatment cells
214 were washed, trypsinized, and the number of total cells and number of viable cells were
215 counted with the MuseTM Cell Count and Viability Kit, as described³¹. Each experiment
216 was run in duplicates in three independent experiments. The mean value of each
217 independent experiment was used for statistics which consisted of one-way ANOVA and
218 Dunnett *post hoc* test (SPSS 15.0 software was used). Proliferation data is expressed as
219 percentage of control condition (basal media).

220

221

222 Results and Discussion

223 Proteins are attractive therapeutic molecules but are sensitive to changes in their
224 environment (pH, temperature, ionic force, *etc.*). Pre-clinical studies, using PLGA
225 nanocapsules loaded with pro-angiogenic factors, have demonstrated great potential in
226 ischemic treatments by inducing a more efficient revascularization compared to
227 administration of the protein alone^{4,32}. We selected VEGF₁₆₅ as a pro-angiogenic factor
228 that activates endothelial cells by inducing cell proliferation and migration³³. We
229 encapsulated VEGF₁₆₅ into PLGA nanocapsules along with SPIONs, with the aim to
230 improve the accumulation of bioactive protein at a target site under a magnetic field
231 gradient. In fact, despite several studies on the formulation of VEGF₁₆₅ loaded PLGA
232 nanocapsules suitable for intravenous administration^{7,10,34}, very few efforts have been
233 done to achieve local delivery of VEGF₁₆₅, since its distribution in non-targeted tissues
234 may cause unwanted side-effects^{35,36}.

235 The size of the PGLA nanocapsules was measured by re-constitution of the freeze-dried
236 material in MilliQ water (Table. 1). The zeta potential of particles in water was -22 ± 2
237 mV. Particles could be readily re-dispersed in water (Fig. 1) and the suspension was
238 stable without precipitation over a period of three months. Importantly the hydrodynamic
239 size and polydispersity of four different batches were reproducible; the average calculated
240 over five batches was 223 nm with a standard deviation of 10 nm. Nanocapsule size was
241 measured by counting 200 particles by SEM. The average diameter was 165 nm with
242 20% polydispersity (Fig. 2), which is considered to be suitable for intravenous
243 administration³⁷.

244 Cryo-TEM confirmed that SPION encapsulation had occurred, with uniform magnetic
245 nanoparticle distribution (visible as black spots in Fig. 3a) within the polymeric matrix.
246 Moreover, the analysis showed a vitrified aqueous dispersion of PLGA nanocapsules,
247 which reflect the administration state, with well-defined spherical shape and no particle

248 aggregation (Fig. 3a). Magnetic measurement at 5 K of lyophilized powder showed high
249 saturation magnetization of nanocapsules at around $80 \text{ emu g}^{-1} \text{ Fe}_2\text{O}_3$, a critical parameter
250 in view of magnetic retention (Fig. 3b). Moreover zero-field cooling, field cooling
251 analysis (ZFC-FC) demonstrated the superparamagnetic character of the nanocapsules,
252 and that SPIONs did not aggregate during the encapsulation process since the blocking
253 temperature (T_B) of the nanocapsules (44 K) was very close to the T_B value of SPIONs in
254 aqueous dispersion (46 K; inset Fig. 3b). We have therefore demonstrated that SPIONs
255 are homogeneously dispersed in the polymer matrix, retaining their superparamagnetic
256 behaviour after the encapsulation process. This is an important result, because it indicates
257 the absence of magnetic dipoles and attractive interactions among nanocapsules that
258 would cause embolism during the intravenous administration. Furthermore, our magnetic
259 nanocapsules present a high relaxivity value and they can be used as contrast agents in
260 magnetic resonance imaging (MRI).

261 The starting amount of VEGF₁₆₅ used for PLGA encapsulation is usually between 0.03
262 and 0.1% w/w^{10,38} and the encapsulation efficiency (EE%) is around 70% for particles of
263 300 nm of hydrodynamic diameter¹⁰. For the encapsulation of SPIONs into PLGA
264 nanocapsules, the achieved final concentration was 1.4% w/w¹⁶ in particles of around 200
265 nm in diameter. In our experiments, the initial VEGF₁₆₅ loading was 0.05% w/w, and
266 SPION loading was 1.8% w/w (expressed as iron weight over PLGA mass used for the
267 encapsulation). We achieved a VEGF EE% value of up to 58% and a SPION EE% value
268 of up to 68% (Table 1), which are both in good agreement with the literature values^{10,16}.

269 With a simple experiment, we checked the magnetic retention of the nanocapsules by
270 application of an external magnetic field. We placed an FeNdB permanent magnet (0.4 T)
271 3 mm away from the colloidal magnetic suspension contained in an Eppendorf tube and
272 after 24 h, we saw retention of the nanocapsules on the plastic wall close to the magnet
273 (Fig. 4). This experiment was a “proof of concept” of the potential of VEGF₁₆₅- and

274 SPION-loaded PLGA nanocapsules' use as magnetic guiding tools to achieve targeted
275 drug delivery. Previous experiments that used microparticles loaded with only 1% w/w
276 iron oxide, demonstrated a magnetic retention effect in rodents' knees, which suggests
277 that our VEGF magnetic nanocapsules may have adequate properties for magnetic
278 targeting³⁹, considering that our average amount of loaded iron oxide is $1.16\% \pm 0.8$
279 ($n=5$).

280 From MRI measurements, we found optimal T_2 relaxation properties of SPION-loaded
281 PLGA nanoparticles with an average transverse relaxivity value (r_2) of $181 \pm 37 \text{ mM}^{-1} \text{ s}^{-1}$,
282 calculated over four different batches (Table 2). Figure 5 shows T_2 weighted phantoms
283 with hypointense signal decay in a concentration-dependent manner. Such high relaxivity
284 value confirms the theranostic character of our nanocapsules, suggesting that it would be
285 possible to track them *in vivo* by MRI.

286 Protein release experiments resulted in a sustained VEGF₁₆₅ release with almost 35% of
287 the total cargo discharged over a period of two weeks; the process was faster during the
288 first hours (Fig. 6).

289 Finally, we demonstrate that recombinant human VEGF₁₆₅ remained bioactive after the
290 encapsulation and subsequent release process. We used the collected media from the
291 VEGF₁₆₅ release study to prove human cerebral microvascular endothelial cell
292 proliferation *in vitro*. Figure 7 shows that the number of cells, treated with release media
293 from VEGF₁₆₅ and SPION-loaded PLGA nanocapsules, was significantly increased
294 compared to control medium (SPION-loaded nanocapsules without VEGF₁₆₅) and basal
295 medium. The highest cell proliferation occurred with release media collected at 1 and 6 h,
296 compared to both control conditions. Release media obtained at 2, 6, and 14 days also
297 induced cell proliferation, although to a lesser extent. This decrease in bioactivity might
298 be explained by partial protein inactivation over time in acidic pH which arises from
299 hydrolytic degradation of PLGA, or by the short protein half-life at 37°C.

300 Cell viability was not affected by our treatments since all conditions presented a mean
301 number of viable cells over 90%. In particular, viability percentages vs. total cells were
302 94 ± 2 for basal media, 94 ± 1 for control nanocapsules without VEGF, 94 ± 2 for VEGF
303 release at 1 h, 96 ± 1 for VEGF release at 6 h, 93 ± 1 for VEGF release at 2 days, 94 ± 1
304 for VEGF release at 6 days, and 92 ± 2 for VEGF release at 14 days.

305

306 **Conclusions**

307 By means of a double-emulsion–solvent-evaporation method, we synthesized PLGA
308 nanocapsules which contained human recombinant VEGF₁₆₅ in their inner particle core
309 and SPIONs embedded in their polymeric layer. The nanocapsules were spherical, very
310 monodisperse, with a hydrodynamic diameter of around 220 nm that is suitable for
311 intravenous administration and good encapsulation efficiencies of both VEGF₁₆₅ and
312 SPIONs. Importantly, the particles were magnetically retained under an applied magnetic
313 field gradient, showed sustained protein release over time and *in vitro* pro-angiogenic
314 activity by inducing human microvascular brain endothelial cell proliferation. We suggest
315 that the co-encapsulation of VEGF₁₆₅ and SPIONs in different compartments of the same
316 formulation (PLGA nanocapsule) may be a promising strategy for developing new
317 targeted therapeutic treatments to enhance angiogenesis.

318

319 **Acknowledgments**

320 This work was partially funded by the Spanish Government, MINECO project:
321 MAT2012-35324, Instituto de Salud Carlos III project: PI10/00694, and co-financed by
322 the European Regional Development Fund (ERDF), and the Generalitat de Catalunya
323 projects: 2014SGR123 and 2014SGR686. A. Rosell is supported by the Miguel Servet
324 program (CP09/00265) of the Instituto de Salud Carlos III. COST Action MP1202 is also
325 gratefully acknowledged.

326

327 **References**

- 328 1. S. Di Santo, Z. Yang, M. Wyler von Ballmoos, J. Voelzmann, N. Diehm, I. Baumgartner and C.
329 Kalka, *PLoS one*, 2009, **4**, e5643.
- 330 2. A. Rosell, A. Morancho, M. Navarro-Sobrino, E. Martinez-Saez, M. Hernandez-Guillamon, S.
331 Lope-Piedrafita, V. Barcelo, F. Borrás, A. Penalba, L. Garcia-Bonilla and J. Montaner, *PLoS one*,
332 2013, **8**, e73244.
- 333 3. E. Carenza, V. Barcelo, A. Morancho, L. Levander, C. Boada, A. Laromaine, A. Roig, J. Montaner
334 and A. Rosell, *Nanomedicine : nanotechnology, biology, and medicine*, 2014, **10**, 225-234.
- 335 4. E. Bible, O. Qutachi, D. Y. Chau, M. R. Alexander, K. M. Shakesheff and M. Modo, *Biomaterials*,
336 2012, **33**, 7435-7446.
- 337 5. F. R. Formiga, B. Pelacho, E. Garbayo, G. Abizanda, J. J. Gavira, T. Simon-Yarza, M. Mazo, E.
338 Tamayo, C. Jauquicoa, C. Ortiz-de-Solorzano, F. Prosper and M. J. Blanco-Prieto, *Journal of*
339 *controlled release : official journal of the Controlled Release Society*, 2010, **147**, 30-37.
- 340 6. Z. S. Patel, H. Ueda, M. Yamamoto, Y. Tabata and A. G. Mikos, *Pharmaceutical research*, 2008,
341 **25**, 2370-2378.
- 342 7. J. S. Golub, Y. T. Kim, C. L. Duvall, R. V. Bellamkonda, D. Gupta, A. S. Lin, D. Weiss, W. Robert
343 Taylor and R. E. Gulberg, *American journal of physiology. Heart and circulatory physiology*,
344 2010, **298**, H1959-1965.
- 345 8. T. Rhim, D. Y. Lee and M. Lee, *Pharmaceutical research*, 2013, **30**, 2429-2444.
- 346 9. N. Ferrara and R. S. Kerbel, *Nature*, 2005, **438**, 967-974.
- 347 10. J. Davda and V. Labhasetwar, *Journal of Biomedical Nanotechnology*, 2005, **1**, 74-82.
- 348 11. A. des Rieux, B. Ucakar, B. P. Mupendwa, D. Colau, O. Feron, P. Carmeliet and V. Preat, *Journal*
349 *of controlled release : official journal of the Controlled Release Society*, 2011, **150**, 272-278.
- 350 12. C. Borselli, F. Ungaro, O. Oliviero, I. D'Angelo, F. Quaglia, M. I. La Rotonda and P. A. Netti,
351 *Journal of Biomedical Materials Research - Part A*, 2010, **92**, 94-102.
- 352 13. J. Kim, L. Cao, D. Shvartsman, E. A. Silva and D. J. Mooney, *Nano Lett*, 2011, **11**, 694-700.
- 353 14. X. Liu, M. D. Kaminski, H. Chen, M. Torno, L. Taylor and A. J. Rosengart, *Journal of controlled*
354 *release : official journal of the Controlled Release Society*, 2007, **119**, 52-58.
- 355 15. L. N. Okassa, H. Marchais, L. Douziech-Eyrolles, K. Herve, S. Cohen-Jonathan, E. Munnier, M.
356 Souce, C. Linassier, P. Dubois and I. Chourpa, *European journal of pharmaceuticals and*
357 *biopharmaceutics : official journal of Arbeitsgemeinschaft fur Pharmazeutische Verfahrenstechnik*
358 *e.V.*, 2007, **67**, 31-38.
- 359 16. Y. Wang, Y. W. Ng, Y. Chen, B. Shuter, J. Yi, J. Ding, S. c. Wang and S. S. Feng, *Advanced*
360 *Functional Materials*, 2008, **18**, 308-318.
- 361 17. L. L. Estevanato, J. R. Da Silva, A. M. Falqueiro, E. Mosiniewicz-Szablewska, P. Suchocki, A. C.
362 Tedesco, P. C. Morais and Z. G. Lacava, *International journal of nanomedicine*, 2012, **7**, 5287-
363 5299.
- 364 18. N. Butoescu, C. A. Seemayer, M. Foti, O. Jordan and E. Doelker, *Biomaterials*, 2009, **30**, 1772-
365 1780.

- 366 19. M. Hamoudeh, R. Diab, H. Fessi, C. Dumontet and D. Cuchet, *Drug development and industrial*
367 *pharmacy*, 2008, **34**, 698-707.
- 368 20. F. Ye, A. Barrefelt, H. Asem, M. Abedi-Valuggerdi, I. El-Serafi, M. Saghafian, K. Abu-Salah, S.
369 Alrokayan, M. Muhammed and M. Hassan, *Biomaterials*, 2014, **35**, 3885-3894.
- 370 21. N. Butoescu, O. Jordan, A. Petri-Fink, H. Hofmann and E. Doelker, *Journal of microencapsulation*,
371 2008, **25**, 339-350.
- 372 22. Q. T. H. Shubhra, H. Mackova, D. Horak, A. Fodor-Kardos, J. Toth, J. Gyenis and T. Feczko, *e-*
373 *Polymers*, 2013.
- 374 23. Q. T. Shubhra, A. F. Kardos, T. Feczko, H. Mackova, D. Horak, J. Toth, G. Dosa and J. Gyenis,
375 *Journal of microencapsulation*, 2014, **31**, 147-155.
- 376 24. A. Z. Faranesh, M. T. Nastley, C. Perez de la Cruz, M. F. Haller, P. Laquerriere, K. W. Leong and
377 E. R. McVeigh, *Magnetic resonance in medicine : official journal of the Society of Magnetic*
378 *Resonance in Medicine / Society of Magnetic Resonance in Medicine*, 2004, **51**, 1265-1271.
- 379 25. M. Mahmoudi, I. Lynch, M. R. Ejtehadi, M. P. Monopoli, F. B. Bombelli and S. Laurent, *Chemical*
380 *reviews*, 2011, **111**, 5610-5637.
- 381 26. T. Cedervall, I. Lynch, S. Lindman, T. Berggard, E. Thulin, H. Nilsson, K. A. Dawson and S. Linse,
382 *Proceedings of the National Academy of Sciences of the United States of America*, 2007, **104**, 2050-
383 2055.
- 384 27. H. Shearer, M. J. Ellis, S. P. Perera and J. B. Chaudhuri, *Tissue engineering*, 2006, **12**, 2717-2727.
- 385 28. D. Blanco and M. J. Alonso, *European journal of pharmaceuticals and biopharmaceutics : official*
386 *journal of Arbeitsgemeinschaft für Pharmazeutische Verfahrenstechnik e.V.*, 1998, **45**, 285-294.
- 387 29. B. B. Weksler, E. A. Subileau, N. Perriere, P. Charneau, K. Holloway, M. Leveque, H. Tricoire-
388 Leignel, A. Nicotra, S. Bourdoulous, P. Turowski, D. K. Male, F. Roux, J. Greenwood, I. A.
389 Romero and P. O. Couraud, *FASEB journal : official publication of the Federation of American*
390 *Societies for Experimental Biology*, 2005, **19**, 1872-1874.
- 391 30. A. B. Ennett, D. Kaigler and D. J. Mooney, *Journal of biomedical materials research. Part A*, 2006,
392 **79**, 176-184.
- 393 31. E. Carenza, V. Barcelo, A. Morancho, J. Montaner, A. Rosell and A. Roig, *Acta Biomater*, 2014,
394 **10**, 3775-3785.
- 395 32. H. Chen, F. Spagnoli, M. Burris, W. B. Rolland, A. Fajilan, H. Dou, J. Tang and J. H. Zhang,
396 *Stroke; a journal of cerebral circulation*, 2012, **43**, 884-887.
- 397 33. A. Hoeben, B. Landuyt, M. S. Highley, H. Wildiers, A. T. Van Oosterom and E. A. De Bruijn,
398 *Pharmacological reviews*, 2004, **56**, 549-580.
- 399 34. J. L. Cleland, E. T. Duenas, A. Park, A. Daugherty, J. Kahn, J. Kowalski and A. Cuthbertson,
400 *Journal of Controlled Release*, 2001, **72**, 13-24.
- 401 35. L. Brannon-Peppas and J. O. Blanchette, *Adv Drug Deliv Rev*, 2004, **56**, 1649-1659.
- 402 36. P. Carmeliet, *Oncology*, 2005, **69 Suppl 3**, 4-10.
- 403 37. R. Gref, M. Lück, P. Quellec, M. Marchand, E. Dellacherie, S. Harnisch, T. Blunk and R. H.
404 Müller, *Colloids and Surfaces B: Biointerfaces*, 2000, **18**, 301-313.
- 405 38. T. Simon-Yarza, F. R. Formiga, E. Tamayo, B. Pelacho, F. Prosper and M. J. Blanco-Prieto,
406 *International journal of pharmaceuticals*, 2013, **440**, 13-18.

- 407 39. N. Butoescu, C. A. Seemayer, G. Palmer, P. A. Guerne, C. Gabay, E. Doelker and O. Jordan,
408 *Arthritis research & therapy*, 2009, **11**, R72.
409
410
411

412

413 **Table 1:** Characterization of samples synthesized by double emulsion-solvent evaporation
 414 method, containing VEGF₁₆₅ and SPIONs (from RG502_23 to RG502_25) and just with SPIONs
 415 (RG502_26, 27). VEGF₁₆₅ amount in PLGA nanocapsules was measured by means of ELISA
 416 immunoassay. SPION content was determined by SQUID measurements. EE%= entrapment
 417 efficiency %; NCs= nanocapsules.

418

419

SAMPLE	PROTEIN	PROTEIN	PROTEIN/NCs	SPIONs	SPION/NCs	SYNTHESIS	DIAMETER
		EE%	(ng·mg ⁻¹)	EE%	(μg·mg ⁻¹)	YIELD%	(DLS, nm)
RG502_23	VEGF	58%	279	60%	10.8	62%	235 (17% PD)
RG502_24	VEGF	57%	273	60%	10.8	63%	225 (17% PD)
RG502_25	VEGF	44%	211	68%	12.2	68%	230 (18% PD)
RG502_26	–	–	–	57%	10.3	65%	215 (17% PD)
RG502_27	–	–	–	65%	11.7	63%	210 (15% PD)

420

421

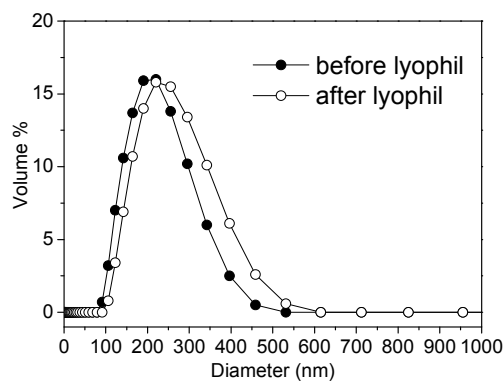
422 **Table 2:** r_2 ($\text{mM}^{-1} \text{s}^{-1}$) values obtained by MRI analysis of lyophilized SPIONs and VEGF₁₆₅-
423 loaded PLGA nanocapsules in agarose. Samples RG502_23, 24, and 25 contain VEGF₁₆₅ and
424 SPIONs. Sample RG502_27 contains only SPIONs.
425

Sample	r_2 ($\text{mM}^{-1} \text{s}^{-1}$)
RG502_23	180
RG502_24	130
RG502_25	201
RG502_27	213

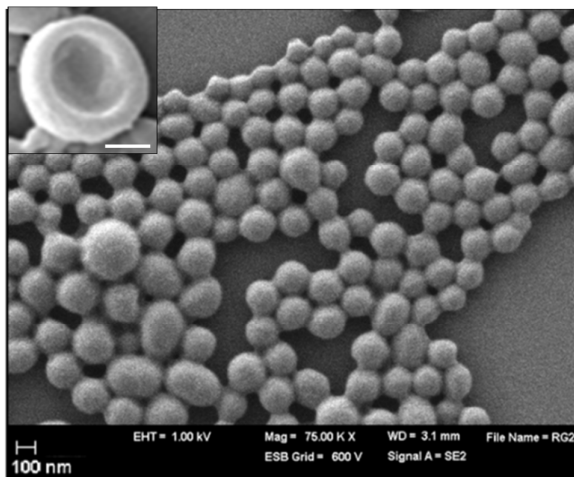
426

427

428 **Figure 1:** DLS measurements of as-synthesized nanocapsules in water (before lyophilization)
429 with mean diameter of 225 nm and 17% polydispersity (black full circles); nanocapsules after
430 freeze-drying and re-dispersion in water with mean diameter of 256 nm and 18% polydispersity
431 (black empty circles).
432
433
434



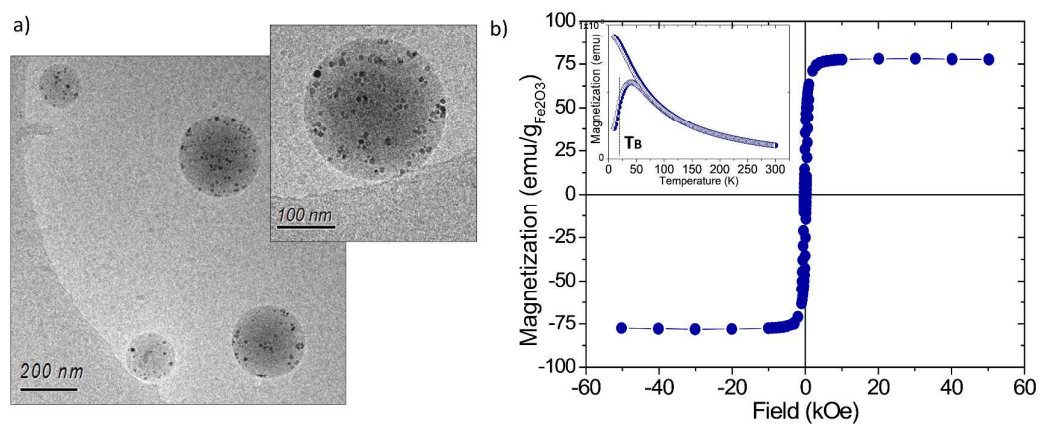
435 **Figure 2:** SEM image of PLGA nanocapsules synthesized by double emulsion-solvent
436 evaporation method, with inset showing the empty inner core of a nanocapsule. Scale bar in the
437 inset of 100 nm.
438
439
440



441

442

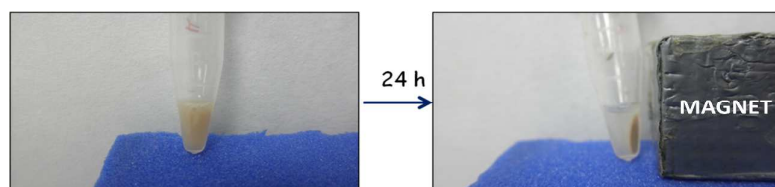
443 **Figure 3:** SPIONs embedded in PLGA nanocapsules: a) Cryo-TEM images of PLGA
444 nanocapsules dispersion in water. Images show spherical nanocapsules with SPIONs visible as
445 black spots, uniformly dispersed in the polymer matrix; b) magnetic measurement of a lyophilized
446 batch RG502_23 at 5 K, showing high saturation magnetization ($78 \text{ emu g}_{\text{Fe}_2\text{O}_3}^{-1}$). ZFC-FC
447 measurement (inset) with a blocking temperature of 44 K.
448
449
450



451

452

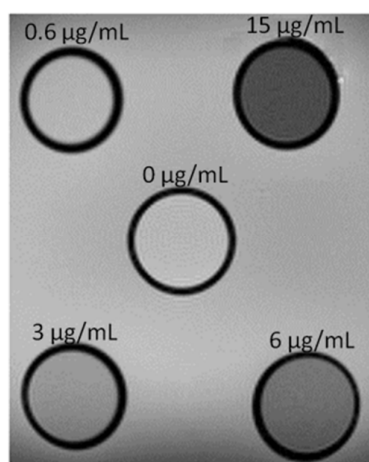
453 **Figure 4:** Eppendorf with 0.2 mL of SPION-loaded PLGA nanocapsules at a concentration of 17
454 mg mL^{-1} . A strong magnet (dimensions $5 \times 5 \times 2$ cm, field 0.4 T) was placed near the Eppendorf.
455 After 24 h, particles adhered to the wall close to the magnet.
456



457

458

459 **Figure 5:** T_2 -weighted phantoms obtained by mixing lyophilized SPION-loaded PLGA
460 nanocapsules with agarose at increasing iron concentrations. The image corresponds to phantoms
461 of sample RG502_23.
462



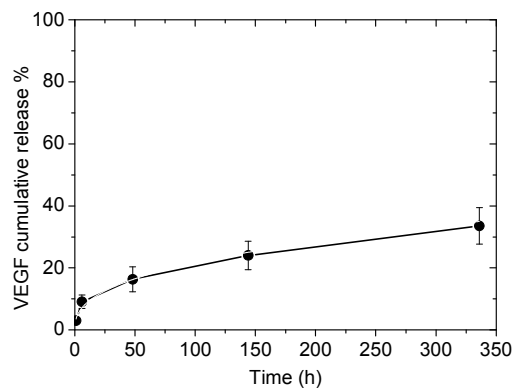
463

464

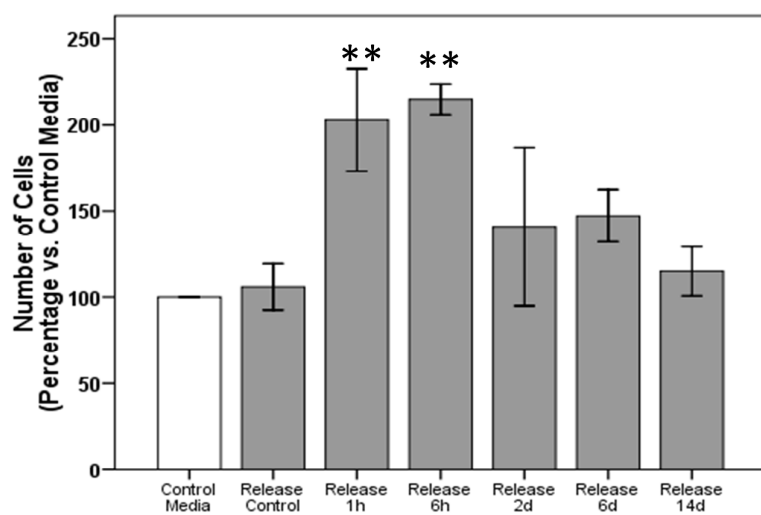
465 **Figure 6:** Protein release curve over a period of two weeks for nanocapsules loaded with VEGF₁₆₅
466 and SPIONs (ELISA immunoassay). The release is expressed as the average of three samples
467 analyzed at the same time; error bars indicate standard deviation. Aliquots were taken after 1 and
468 6 h, 2, 6, and 14 days.
469
470

471

472



473 **Figure 7:** Bar graphs representing the percentage of endothelial cells in each treatment condition
474 vs. control treatment (basal media). Bars represent mean \pm SD of n=3 independent experiments.
475 ** p<0.001.
476



477

1

Table of contents

2

New drug delivery systems based on biodegradable magnetic nanocapsules for targeted delivery of pro-angiogenic proteins, potentially useful in therapeutic angiogenesis.

3

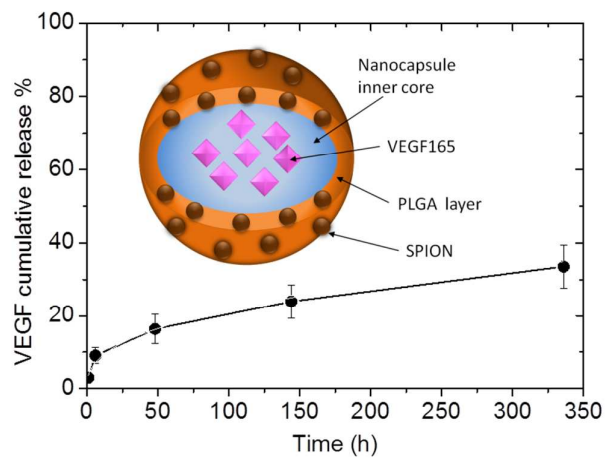
4

5

6

Graphical Abstract

7



8